Two-Dimensional Structure and Particle Pinch in Tokamak H Mode

Naohiro Kasuya and Kimitaka Itoh
National Institute for Fusion Science, Toki, Gifu 509-5292, Japan
(Received 16 November 2004; published 16 May 2005)

Two-dimensional structures of the electrostatic potential, density, and flow velocity near the edge of a tokamak plasma are investigated. The model includes the nonlinearity in bulk-ion viscosity and turbulence-driven shear viscosity. For the case with the strong radial electric field (H mode), a two-dimensional structure in a transport barrier is obtained, giving a poloidal shock with a solitary radial electric field profile. The inward particle pinch is induced from this poloidal asymmetric electric field, and increases as the radial electric field becomes stronger. The abrupt increase of this inward ion and electron flux at the onset of L- to H-mode transition explains the rapid establishment of the density pedestal, which is responsible for the observed spontaneous self-reorganization into an improved confinement regime.

DOI: 10.1103/PhysRevLett.94.195002 PACS numbers: 52.55.Fa, 52.25.Fi, 52.55.Dy

Turbulent transport in high temperature confined plasmas has become one of the most challenging issues in plasma physics. In particular, the formation of transport barriers in toroidal plasmas has been the focus of research [1]. A typical example of this is H-mode transition [2]. Key mechanisms to understand the H-mode transition include bifurcation of the electric field [3,4] and associated suppression of turbulence by electric field structures [5,6]. Thus significant attention has been devoted to studying the steep radial electric field structure in the L-H transition physics [7]. The nonlinear formation mechanism of the radial electric field structure has been studied with biased limiter experiments in which externally driven H-mode transition was induced [8,9]. Theoretical studies have clarified the formation mechanism of the solitary radial electric field structure [10,11]. The nonlinearity in the relationship between the radial electric field and the radial current has been examined explicitly in other toroidal plasma experiments [12].

Although significant progress towards understanding the radial electric field structure has been made, there still remain fundamental issues. For instance, the rapid establishment of the density profile pedestal after the onset of the L-H transition [13] remains unexplained. It is well known that turbulent diffusivity decreases rapidly after transition. However, this reduced diffusion makes the time for reaching a steady state much longer than observed. Another issue is the formation of a poloidal shock associated with the large poloidal flow. Theories have predicted, in which only poloidal variation was taken and a radial structure was neglected, that the poloidal shock can appear in H-mode plasmas [14,15]. Some experiments have indicated poloidal asymmetry [16]. If such a poloidal shock exists, a large inward particle pinch could be induced [1], and may influence the pedestal formation. This consideration motivates the study of two-dimensional structure at the transport barrier. Some progress has been reported [17,18], but the understanding is far from satisfactory.

In this Letter, we study the two-dimensional structure of the electrostatic potential, density, and flow velocity near the edge of a tokamak plasma. A set of equations, which describes the transition to the steep radial electric field structure as well as poloidal inhomogeneity, is derived by considering the nonlinearity in bulk-ion viscosity and (turbulence-driven) shear viscosity. The poloidal asymmetric structure generates inward particle pinch, and gives an explanation for a rapid establishment of the edge pedestal on the L-H transition.

We consider a large aspect ratio tokamak where a circular cross section and the coordinates r, θ, and ζ are used (r, radius; θ, poloidal angle; ζ, toroidal angle). Poloidal variations of the density and the electrostatic potential are considered, but that of the temperature is neglected. Electrons are isothermal, ions are adiabatic, and $n_i = n_e \equiv n$ is taken, where n_i and n_e are the ion and electron density, respectively. Derivation of the model equation follows Ref. [14], but the radial flow and shear viscosity are taken into account here [19]. By these terms, radial and poloidal structures are coupled with each other. The structures are governed by the momentum balance equation,

$$m_i n \frac{d}{dt}\vec{V}_i = \vec{J}\times\vec{B} - \vec{\nabla}(p_i + p_e) - (\vec{\nabla}\cdot\overleftrightarrow{\pi}_i)_{\text{bulk}} - (\vec{\nabla}\cdot\overleftrightarrow{\pi}_i)_{\text{shear}}, \tag{1}$$

where $\vec{V}_i$ is the flow velocity, $\vec{J}$ is the plasma current, p_i and p_e are the ion and electron pressures, $\overleftrightarrow{\pi}_i$ is the viscosity tensor of ions, and m_i is the ion mass. Pressure $p = nT$, and constant temperature T is assumed. The viscosity is divided into two terms: bulk viscosity given by a neoclassical process [20], and shear viscosity given by an anomalous process [1]. The viscosity of electrons is neglected because it is smaller by a factor of the order of $\sqrt{m_e/m_i}$. The flow velocity is written as $\vec{V} = \vec{V}_\parallel + \frac{\vec{E}\times\vec{B}}{B^2} = (-\frac{I}{rRB^2}\times \frac{\partial\Phi}{\partial\theta}, \frac{KB_{\text{p}}}{n}, \frac{KB_\zeta}{n} - \frac{1}{B_{\text{p}}}\frac{\partial\Phi}{\partial r})$, where Φ is the electrostatic potential, $K = nV_{\text{p}}/B_{\text{p}}$ corresponding to the poloidal flow, and $I = R^2\vec{B}\cdot\nabla\zeta$. The toroidal symmetry is utilized in this description. The parallel component and averaged poloidal component of the momentum balance Eq. (1) are given to be

$$-\frac{nI}{KB^2rR}\frac{\partial\Phi}{\partial\theta}\frac{\partial}{\partial r}\left[\frac{1}{2}\left(\frac{KB}{n}\right)^2\right]+\frac{B_\mathrm{p}}{r}\frac{\partial}{\partial\theta}\left[\frac{1}{2}\left(\frac{KB}{n}\right)^2\right]+\frac{IB_\zeta}{B^2rR}\frac{\partial\Phi}{\partial\theta}\frac{\partial}{\partial r}\left[\frac{I}{RB_\mathrm{p}B_\zeta}\frac{\partial\Phi}{\partial r}\right]-\frac{KB_\mathrm{p}B_\zeta}{nr}\frac{\partial}{\partial\theta}\left[\frac{I}{RB_\mathrm{p}B_\zeta}\frac{\partial\Phi}{\partial r}\right]$$
$$=-\frac{B_\mathrm{p}}{m_ir}\frac{\partial}{\partial\theta}\left(\frac{\langle p_e\rangle}{\langle n\rangle}\ln n+\frac{5}{2}\frac{\langle p_\mathrm{i}\rangle}{\langle n^{5/3}\rangle}n^{2/3}\right)-\frac{1}{m_in}(\vec{B}\cdot\vec{\nabla}\cdot\overleftrightarrow{\pi}_i)_\mathrm{bulk}-\frac{1}{m_in}(\vec{B}\cdot\vec{\nabla}\cdot\overleftrightarrow{\pi}_i)_\mathrm{shear}, \quad (2)$$

$$\left\langle-\frac{nI}{KB^2rR}\frac{\partial\Phi}{\partial\theta}\frac{\partial}{\partial r}\left[\frac{1}{2}\left(\frac{KB_\mathrm{p}}{n}\right)^2\right]+\frac{B_\mathrm{p}}{r}\frac{\partial}{\partial\theta}\left[\frac{1}{2}\left(\frac{KB_\mathrm{p}}{n}\right)^2\right]\right\rangle=\frac{1}{m_i}\left\langle\frac{JB_\mathrm{p}B_\zeta}{n}\right\rangle-\frac{1}{m_i}\left\langle\frac{\vec{B}_\mathrm{p}\cdot\vec{\nabla}\cdot\overleftrightarrow{\pi}_i}{n}\right\rangle_\mathrm{bulk}-\frac{1}{m_\mathrm{i}}\left\langle\frac{\vec{B}_\mathrm{p}\cdot\vec{\nabla}\cdot\overleftrightarrow{\pi}_i}{n}\right\rangle_\mathrm{shear}, \quad (3)$$

where $\langle\ \rangle$ denotes the flux surface average. The radial flow is taken into account, so $\partial\Phi/\partial\theta$ terms are involved in the left side of Eqs. (2) and (3). Using the viscosity tensor $\overleftrightarrow{\pi}_i = (p_\parallel - p_\perp)(\hat{b}\,\hat{b} - \overleftrightarrow{I}/3)$, where $(p_\parallel - p_\perp)$ is the pressure anisotropy and $\hat{b}$ is the unit vector parallel to the magnetic field, the bulk viscosity term can be written as

$$(\vec{B}\cdot\vec{\nabla}\cdot\overleftrightarrow{\pi}_i)_\mathrm{bulk}=\frac{2}{3}\frac{B_\mathrm{p}}{r}\frac{\partial}{\partial\theta}(p_\parallel-p_\perp)-(p_\parallel-p_\perp)\frac{B_\mathrm{p}}{B}\frac{1}{r}\frac{\partial B}{\partial\theta}. \quad (4)$$

The first term of Eq. (4) is dominant, so only this term is kept in Eq. (2) hereafter. In contrast, the surface average is taken in Eq. (3), in which the second of Eq. (4) remains. The pressure anisotropy was rewritten in terms of B and n in Ref. [21], and the explicit form is not reproduced here. The shear viscosity is given by the second derivative of the flow velocity, and here simply given to be

$$(\vec{B}\cdot\vec{\nabla}\cdot\overleftrightarrow{\pi}_i)_\mathrm{shear}=-m_in\mu\vec{B}\cdot\nabla_\perp{}^2\vec{V}, \quad (5)$$

where μ is a shear viscosity coefficient. The coefficient μ depends on the radial electric field and has spatial variation, but we take it as constant in space for simplicity. The Boltzmann relation

$$n=\bar{n}\exp\left(\frac{e\Delta\Phi}{T_i}\right) \quad (6)$$

is adopted here to determine variables, where $\bar{f}$ and Δf represent the spatial average and perturbed parts of quantity f, respectively. The variables that must be determined from Eqs. (2), (3), and (6) are K, Φ, and n, which have radial and poloidal variations. A new variable $\chi \equiv \ln(n/\bar{n})$ is introduced, which is directly related to the potential perturbation with Eq. (6).

The case when the poloidal Mach number $M_\mathrm{p} \sim 1$ [$M_\mathrm{p} = E_\mathrm{r}/(\mathrm{v_{ti}}B_\mathrm{p})$, where $\mathrm{v_{ti}}$ is the thermal velocity of ions] is the main interest in this Letter, and the shock ordering, which is $\chi = O(\varepsilon^{1/2})$, is adopted, where ε is the inverse aspect ratio. ε is taken to be small because the calculation is carried out only near the edge in a large aspect ratio tokamak. A condition $V_\mathrm{r}/V_\mathrm{p} \ll 1$ is satisfied, even if the strong poloidal shock exists. This condition is confirmed, *a posteriori,* by the derived structures. The condition $V_\mathrm{r}/V_\mathrm{p} \ll 1$ makes the model equation simpler. The continuity equation in a steady state $\mathrm{div}(nV) = 0$ shows K is a flux surface variable. Expanding Eq. (2) with χ, and taking up to $O(\varepsilon)$, the following model equation is obtained:

$$-\hat{\mu}r^2\frac{B_0}{B_\mathrm{p}}\frac{\partial^2}{\partial r^2}\{M_\mathrm{p}[\exp(-\chi)-1]\}+\frac{2}{3}D\exp(-\chi)\frac{\partial^2\chi}{\partial\theta^2}+(1-M_\mathrm{p}{}^2)\frac{\partial\chi}{\partial\theta}+2A\frac{\partial\chi^2}{\partial\theta}$$
$$=\varepsilon\left(\left\{D-\hat{\mu}\frac{B_0}{B_\mathrm{p}}\left[2r^2\frac{\partial^2M_\mathrm{p}}{\partial r^2}+4r\frac{\partial}{\partial r}M_\mathrm{p}-2M_\mathrm{p}\right]\right\}\cos\theta-2M_\mathrm{p}{}^2\sin\theta\right), \quad (7)$$

where $M_\mathrm{p} = KB_0/(\bar{n}\mathrm{v_{ti}}C_\mathrm{r})$, $\hat{\mu} = \mu/(r\mathrm{v_{ti}}C_\mathrm{r})$, $A = M_\mathrm{p}{}^2/2 + 5/(36C_\mathrm{r}{}^2)$, $C_\mathrm{r}{}^2 = (5/3 + T_e/T_i)/2$, $D = 4\sqrt{\pi}I_\mathrm{ps}KB_0/(3\bar{n}\mathrm{v_{ti}}C_\mathrm{r}{}^2)$, and I_ps defined in Ref. [14] has nonlinear dependency on M_p. (This is the equation for a strong toroidal damping case when $M_\mathrm{p} = [I/(\mathrm{v_{ti}}B_0B_\mathrm{p}C_\mathrm{r}R)](\partial\Phi/\partial r)$. In this case M_p is proportional to the radial electric field.) Now Eqs. (3), (6), and (7) determine the structure. This set is solved as follows: A profile of M_p is obtained by solving Eq. (3) independently from Eq. (7). Equation (3) is the same as the equation used for obtaining a radial profile of the radial electric field in the previous H-mode transition model. M_p (including the radial profile) is put into Eq. (7), and the two-dimensional structure of χ is obtained. Then the radial velocity is deduced.

Using these model equations, analysis is carried out in the region near the plasma edge, $r = (a - d) \sim a$, where $r = a$ is the position of the last closed flux surface. We consider the case that the strong radial electric field is self-organized in the middle region of this domain, and choose the boundary condition to be $\chi = 0$ at $r = (a - d)$ and a. This is an idealization that no perturbation exists outside of this region (such as the edge barrier or biased region). Equation (7) is solved with the given M_p profile, which has been obtained in literature [11]. (In performing calculations examples of parameters are chosen as $R = 1.75$[m], $a = 0.46$[m], $B_0 = 2.35$[T], $T_i = 40$[eV], $I_\mathrm{p} = 200$[kA], and the boundaries $r - a = 0, -5$[cm].)

We first study the case that M_p is homogeneous to clarify the competition between the steepening by the $(V\cdot\nabla)V$ nonlinearity and the radial diffusion. In the absence of shear viscosity, the poloidal shock is predicted to appear as was given in [14]. When the shear viscosity exceeds a

threshold value $\hat{\mu} > \mu_{\rm ib} = Dd^2 B_{\rm p}/(12a^2 M_{\rm p} B_0)$, Eq. (7) can be simplified and have a solution to be

$$\chi(r,\theta) = \frac{\varepsilon\sqrt{D^2 + 4{M_{\rm p}}^4}}{2\hat{\mu}a^2 M_{\rm p}} \frac{B_{\rm p}}{B_0}(r-a)(r-a+d)\sin(\theta+\theta_\alpha), \tag{8}$$

for the intermediate regime. χ is inversely proportional to μ in this regime. Equation (8) gives the maximum of χ at the point $\theta = \pi/2 + \theta_\alpha$, where $\tan\theta_\alpha = -D/(2{M_{\rm p}}^2)$ and the maximum gradient of χ is $(\partial\chi/\partial\theta)_{\rm max} = \varepsilon {\rm v}_{\rm th} C_{\rm r} B_{\rm p} d^2 \sqrt{D^2 + 4{M_{\rm p}}^4}/(8aM_{\rm p}B_0\mu)$ at the point $\theta = \pi - \theta_\alpha$. When the shear viscosity is very strong $\hat{\mu}B_0/B_{\rm p} \gg 1$, we have $\chi(r,\theta) \sim (\varepsilon/a^2)(r-a)(r-a+d)\cos\theta$, which has no dependence on μ and $M_{\rm p}$. In this case, no strong shock appears. In this way, the magnitude of μ determines the two-dimensional structure. Experimentally μ is estimated to be around $10^0[{\rm m}^2/{\rm s}]$ [22,23], and thus we take $\mu = 1[{\rm m}^2/{\rm s}]$ in the following calculation.

We next study the two-dimensional structure by employing the solitary structures of the radial electric field, which appear in the biased electrode experiments or in the H-mode edge barriers. Profiles of $M_{\rm p}$ are shown in Fig. 1, which is taken to illustrate the bifurcation of the radial electric field [11]. Under this condition, Eq. (7) is solved. Figure 2 shows a profile of the poloidal electric field. The region where $M_{\rm p}$ has a large value is localized in the middle of the shear region, so a localized large poloidal electric field exists at the points of the shock in those with large $M_{\rm p}$. In addition, the magnitude of $M_{\rm p}$ varies in the radial direction, and the poloidal position of the shock varies in the radial direction accordingly. We conclude that the two-dimensional structure of the edge transport barrier exists and influences the plasma flow, for the plasma parameters that are relevant to the H-mode confinement.

Comparison of the strong inhomogeneous $E_{\rm r}$ case with the weak homogeneous $E_{\rm r}$ case clarifies the formation of the localized steep two-dimensional structure. The strong $E_{\rm r}$ case has a peaked $E_{\rm r}$ profile in the middle of the calculated region, although the weak $E_{\rm r}$ case has a spatially constant profile. The strong $E_{\rm r}$ case has a large potential perturbation (the maximum value $\Delta\Phi_{\rm max} = 50[{\rm V}]$ in this case) and a localized large poloidal electric field where the poloidal flow shear is strong (the maximum value $E_{\theta\,{\rm max}} = 63[{\rm V/m}]$). This large poloidal electric field generates a large $E \times B$ flow pointing to the radial direction (the maximum value $V_{\rm r\,max} = 28[{\rm m/s}]$). In the weak $E_{\rm r}$ case, each value has $\Delta\Phi_{\rm max} = 4[{\rm V}]$, $E_{\theta\,{\rm max}} = 9[{\rm V/m}]$, and $V_{\rm r\,max} = 4[{\rm m/s}]$, respectively, which are one order smaller than in the strong $E_{\rm r}$ case.

Finally, we discuss the impact of this two-dimensional structure on the formation of the pedestal of the transport barrier. The poloidal structure is found to generate radial flow much larger than $1[{\rm m/s}]$, but this large flow region is poloidally localized and the flow changes its direction according to the poloidal position. We calculate the flux-surface-averaged flux in the radial direction $\langle nV_{\rm r}\rangle = \langle nE_{\rm p}/B\rangle$ by the use of the two-dimensional solution. Figure 3(a) represents the radial profiles of the flux-surface-averaged radial flux in the strong and weak $E_{\rm r}$ cases, respectively. The radial flux has a negative value, so it points inward to the plasma center. Inward flux arises from poloidal asymmetry. Figure 3(b) shows the relationship between the maximum of $M_{\rm p}$ and the particle pinch velocity. A moderate inward pinch velocity $V_{\rm r} \sim 1[{\rm m/s}]$ exists even in the weak $E_{\rm r}$ case (like the L mode). In the strong $E_{\rm r}$ case, which is relevant to the H-mode or biased electrode experiments, a larger radial flow (inward pinch) is induced. It should be noticed that not only the large magnitude of poloidal flow but also the gradient of poloidal flow affect to increase the inward pinch velocity. Figure 3(a) shows that the radial flux has a maximum in the radial position where $M_{\rm p}$ shear is large. That is coming from the form of the shear viscosity Eq. (5) that combines the poloidal asymmetry of the magnetic field B and the gradient and curvature of flow velocity.

The increase of inward convective particle flux has a large impact on the pedestal formation on the L-H transition. In the L-H transition, $M_{\rm p}$ changes abruptly, so that the

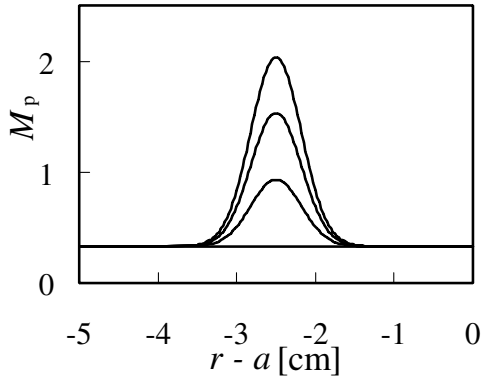

FIG. 1. Solitary radial profiles of $M_{\rm p}$.

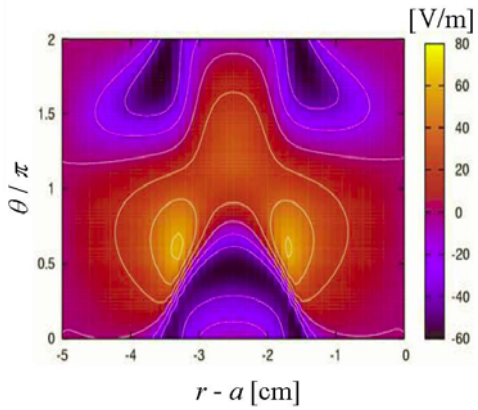

FIG. 2 (color online). Two-dimensional structure of the poloidal electric field with strong and inhomogeneous $E_{\rm r}$. Given $M_{\rm p}$ profile is that with the largest peak height in Fig. 1.

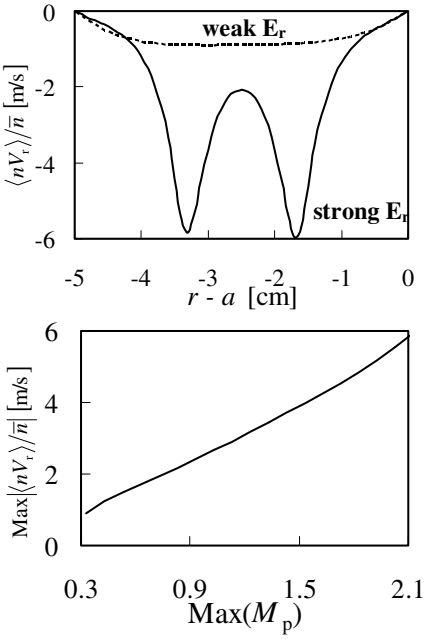

FIG. 3. (a) Radial profiles of flux-surface-averaged particle flux in the case of weak homogeneous and strong inhomogeneous E_r. (b) Relationship between the maximum of M_p and particle pinch velocity. Increase of max(M_p) corresponds to increase of peak height of M_p as shown in Fig. 1.

convective transport changes abruptly in the transport barrier region in the same time. The suppression of transport and the reduction of diffusive transport occurs in the transport barrier. The reduction of the diffusion coefficient explains the steepening of the H-mode pedestal, but the time constant of the pedestal formation is difficult to explain. That is, the necessary time for reaching the final pedestal gradient in the region with the width δ is given by $\tau = \delta^2/D_a$, where D_a is the reduced transport coefficient in the H mode. It takes long time to form the pedestal ($\tau = 25$[ms] when $\delta = 5$[cm] and $D_a = 0.1$[m^2/s]). The H-mode pedestal can be formed in a much shorter time $\tau \ll 10$[ms] [13]. If the convective velocity increases abruptly, the time constant of the pedestal formation is represented to be $\tau = \delta/V_r$ ($\tau = 5$[ms] when $\delta = 5$[cm] and $V_r = 10$[m/s]), so a sudden increase of the inward pinch flux is a candidate for the cause of the rapid H-mode pedestal formation.

In summary, multidimensionality was introduced into H-mode barrier physics in tokamaks. The radial steep structure in the H-mode and the poloidal shock structure with the large poloidal flow were taken into account in a self-sustained system. The model equations with shear viscosity were derived. The magnitude of shear viscosity determines the steepness and the position of the shock structure. In shock ordering, a structure of the flux-surface-averaged part is solved first, and using this M_p profile, a two-dimensional structure can be obtained iteratively. The one-dimensional model that has been used to study the L-H transition condition [7] is validated by this two-dimensional analysis. The radial solitary structure of the strong radial electric field was found to be associated with the poloidal shock structure for the parameters that are relevant to H-mode plasmas. The ion and electron inward pinch flux exists, and has a magnitude of O(1–10)[m/s] in an H-mode transport barrier. An abrupt increase of this convective transport at the onset of the transition was predicted by this theory, which provides a new explanation of rapid H-mode pedestal formation.

The authors acknowledge useful discussions with Professor S.-I. Itoh, Dr. M. Yagi, Professor A. Fukuyama, Professor Y. Takase, and Professor Y. Miura, as well as suggestions by Professor G. R. Tynan. This work is partly supported by the Grant-in-Aid for Specially Promoted Research of MEXT (16002005), by the Grant-in-Aid for Scientific Research of MEXT (15360495), and by the collaboration programs of NIFS and of RIAM of Kyushu University.

[1] K. Itoh, S.-I. Itoh, and A. Fukuyama, *Transport and Structural Formation in Plasmas* (IOP, Bristol, 1999).
[2] F. Wagner *et al.*, Phys. Rev. Lett. **49**, 1408 (1982).
[3] S.-I. Itoh and K. Itoh, Phys. Rev. Lett. **60**, 2276 (1988); S.-I. Itoh and K. Itoh, Nucl. Fusion **29**, 1031 (1989).
[4] K. C. Shaing and E. C. Crume, Phys. Rev. Lett. **63**, 2369 (1989).
[5] S.-I. Itoh and K. Itoh, J. Phys. Soc. Jpn. **59**, 3815 (1990).
[6] H. Biglari, P. H. Diamond, and P. W. Terry, Phys. Fluids B **2**, 1 (1990).
[7] K. Itoh and S. I. Itoh, Plasma Phys. Controlled Fusion **38**, 1 (1996).
[8] R. J. Taylor *et al.*, Phys. Rev. Lett. **63**, 2365 (1989).
[9] R. R. Weynants *et al.*, Nucl. Fusion **32**, 837 (1992).
[10] K. Itoh, S.-I. Itoh, M. Yagi, and A. Fukuyama, Phys. Plasmas **5**, 4121 (1998).
[11] N. Kasuya, K. Itoh, and Y. Takase, Nucl. Fusion **43**, 244 (2003).
[12] A. Fujisawa *et al.*, Phys. Rev. Lett. **79**, 1054 (1997).
[13] F. Wagner *et al.*, in *Proceedings of the Thirteenth International Conference on Plasma Physics and Controlled Nuclear Fusion Research, Washington, 1990* (IAEA, Vienna, 1991), Vol. 1, p. 277.
[14] K. C. Shaing *et al.*, Phys. Fluids B **4**, 404 (1992).
[15] T. Taniuti *et al.*, J. Phys. Soc. Jpn. **61**, 568 (1992).
[16] G. R. Tynan *et al.*, Plasma Phys. Controlled Fusion **38**, 1301 (1996).
[17] M. J. Schaffer *et al.*, Phys. Plasmas **8**, 2118 (2001).
[18] W. M. Stacey, Phys. Plasmas **9**, 3874 (2002).
[19] N. Kasuya, K. Itoh, and Y. Takase, J. Plasma Fusion Res. **6**, 283 (2004).
[20] K. C. Shaing, E. C. Crume, and W. A. Houlberg, Phys. Fluids B **2**, 1492 (1990).
[21] S. P. Hirshman and D. J. Sigmar, Nucl. Fusion **21**, 1079 (1981).
[22] K. Ida and N. Nakajima, Phys. Plasmas **4**, 310 (1997).
[23] N. Kasuya Ph.D. thesis, University of Tokyo, 2003.